A benchmark study on reactive two-phase flow in porous media

Part II - results and discussion

Ahusborde, Etienne; Amaziane, Brahim; de Hoop, Stephan; El Ossmani, Mustapha; Flauraud, Eric; Hamon, François P.; Kern, Michel; Socié, Adrien; Su, Danyang; Mayer, K. Ulrich

DOI
10.1007/s10596-024-10269-y

Publication date
2024

Document Version
Final published version

Published in
Computational Geosciences

Citation (APA)
Ahusborde, E., Amaziane, B., de Hoop, S., El Ossmani, M., Flauraud, E., Hamon, F. P., Kern, M., Socié, A., Su, D., Mayer, K. U., Tóth, M., & Voskov, D. (2024). A benchmark study on reactive two-phase flow in porous media: Part II - results and discussion. *Computational Geosciences*, *28*(3), 395-412. https://doi.org/10.1007/s10596-024-10269-y

Computational Geosciences (2024) 28:395–412
https://doi.org/10.1007/s10596-024-10269-y

ORIGINAL PAPER

A benchmark study on reactive two-phase flow in porous media: Part II - results and discussion

Etienne Ahusborde[1] · Brahim Amaziane[1] · Stephan de Hoop[2] · Mustapha El Ossmani[1,3] · Eric Flauraud[4] · François P. Hamon[5] · Michel Kern[6,7] · Adrien Socié[8] · Danyang Su[8] · K. Ulrich Mayer[8] · Michal Tóth[9] · Denis Voskov[2,10]

Received: 22 March 2023 / Accepted: 3 January 2024 / Published online: 3 February 2024

Abstract
This paper presents and discusses the results obtained by the participants to the benchmark described in de Hoop et al, Comput. Geosci. (2024). The benchmark uses a model for CO_2 geological storage and focuses on the coupling between two-phase flow and geochemistry. Several test cases of various levels of difficulty are proposed, both in one and two spatial dimensions. Six teams participated in the benchmark, each with their own simulation code, though not all teams attempted all the cases. The codes used by the participants are described, and the results obtained on the various test cases are compared, as well as the performance of the codes. It is shown that the results obtained are widely consistent, giving a good level of confidence in the outcome of the benchmark. The general complexity of two-phase flow coupled with chemical reactions altering porous media means that some differences between the codes remain. Besides, from the convergence study, it is clear that the two-dimensional problem has a relatively high sensitivity to a spatial resolution which adds to the complexity.

Keywords Multiphase flow · Reactive transport · Benchmark · Code comparison · Geological carbon storage

1 Introduction

This paper presents and compares the results obtained by the groups who participated in the benchmark test cases described in the companion paper [1].

The main focus of the benchmark was on the interaction between two-phase flow and chemical reactions, mainly the reactions involving the solid matrix. Specific goals of the benchmark are stated in [1]. Accordingly, the physical model is based on a two-phase multicomponent flow with phase changes. The main components are water (H_2O) and carbon dioxide (CO_2), and they can exist in both the liquid and the gas phases. The liquid phase contains other components in the form of ions that can react between themselves and the rock matrix. In order to focus on the specific challenges listed in [1] the physics has been deliberately kept simple, so that the resulting model has no claim at being in any way a realistic CO_2 storage scenario.

✉ Michel Kern
Michel.Kern@inria.fr

Extended author information available on the last page of the article

We first review the different test cases proposed in [1]. The benchmark comprises five test cases of increasing difficulty: the first two use a 1D geometry, while the remaining three cases are based on a 2D geometry. All but the last test cases are based on a simple chemical system, with only one chemical reaction involving calcite precipitation and dissolution. The last case involves a more complex chemical system.

- Test cases 1.1 and 1.2 are based on a 1D geometry. Gas is injected from the left. Chemistry can be either kinetic or at equilibrium. Because the results of both cases were quite close, only the kinetic case is discussed in this paper. However, because some groups chose to model equilibrium reactions as kinetic reactions with a large kinetic constant, both cases were kept in the benchmark description.
- Test case 2.1 moves to a 2D geometry, with a rectangular domain including a low porosity and permeability zone. Water is injected on the top part of the left boundary, and gas on the bottom part. This test case can be simulated with or without gravity, and the results in both cases are quite different. Because the calcite dissolution

constant is taken artificially high, precipitation and dissolution effects are quite pronounced in this model.
- Test case 2.2 is based on the same geometry as test case 2.1, with gravity, but uses a more complex chemical system that includes the dissociation of water and carbonic dioxide. It also uses a more realistic dissolution constant for calcite. This test stresses the difficulties that will have to be faced when dealing with both a complex flow model and a more complex chemical model.

Six different teams participated in the benchmark, each with their own simulation code. We list the groups and their codes, as each code is presented in more detail later on (see Section 2).

- Université de Pau et des Pays de l'Adour and Inria (UPPA-Inria), with DuMu^X;
- Delft University of Technology (TU-DELFT), with DARTS;
- IFPEN, with CooresFlow;
- University of Heidelberg, with PDELab;
- University of British Columbia (EOAS-UBC), with MIN3P;
- TotalEnergies with Lawrence Livermore National Laboratory and Stanford University (TTE-LLNL-SU), with GEOS.

We compare the results obtained by the different groups, noting that not all cases were attempted by all the groups. The comparison remains at a qualitative level, as the benchmarks did not include specific numerical quantities. We also compare the numerical performance of the different codes, in terms of the number of time steps, as well as number of iterations when iterative methods are used.

The outline of the paper is as follows: in Section 2, the different codes used by the participants to solve the benchmark are introduced. Section 3 then presents the results obtained for the different test cases (there are five cases of increasing complexity). Some conclusions are drawn in Section 4 while Appendix A discusses the grid sensitivity.

2 Description of the codes

2.1 DuMu^X: UPPA-Inria

DuMu^X (DUNE for Multi-{Phase, Component, Scale, Physics, ...} flow and transport in porous media) [2] is a free and open-source simulator for flow and transport processes in porous media, based on the Distributed and Unified Numerics Environment DUNE [3]. DUNE is an object-oriented software written in C++ that handles general input/output, memory management, grid generation and massive parallelism. For several years, UPPA-Inria has implemented various numerical schemes for reactive transport modeling in the DuMu^X framework. More precisely, in [4–6], we developed and integrated a sequential approach that splits the global problem into two sub-problems. The first sub-problem computes a two-phase compositional flow where only species present in both phases are treated implicitly. Exchanges between phases are totally solved in this step and the contribution of the other species is treated explicitly. The second sub-problem calculates a reactive transport problem where flow properties (Darcy velocity for each phase, saturation of each phase, temperature, density of each phase, etc.) are given by the first step. In [4, 5], a sequential iterative approach (SIA) has been implemented for the reactive transport sub-problem while in [6], the SIA was replaced by a global implicit approach to reduce possible time-splitting errors caused by the SIA. More recently we developed in [7, 8] a fully implicit, fully coupled method based on a direct substitution approach. In this contribution, we only present results stemming from the fully implicit approach. Nonetheless, we can mention that a sequential scheme was also used for Test 2.2. The results were very close to the ones obtained for the fully implicit scheme and are not presented.

A cell-centered finite volume (FV) scheme is used for spatial discretization. A fully upwind scheme is used to approximate the numerical flux for the convective term, while a two-point flux approximation (TPFA) calculates the diffusive terms. This is possible because the geometries involved in the benchmark are simple enough to allow for orthogonal meshes to be used. For more general meshes, multi-point flux approximations (MPFA) could be used. The nonlinear system is solved by a Newton-Raphson algorithm where the Jacobian matrix is approximated by numerical differentiation. A BiConjugate Gradient STABilized (BiCGSTAB) method preconditioned by an Algebraic Multigrid (AMG) solver is used to solve the linear systems. Finally, an adaptive time-stepping strategy based on the number of iterations required by the Newton method to achieve convergence for the last time iteration is used. A detailed description of our methodology is given in [8]. This methodology has been validated already by several test cases including high-performance computing and applied to geological storage of CO_2 in deep saline aquifers.

2.2 DARTS: TU-DELFT

DARTS (Delft Advanced Research Terra Simulator) is a scalable parallel open-source simulation framework for modeling industrial and academic energy transition applications [9]. It combines the high efficiency of the C++ kernel with the flexibility of the Python interface, which makes DARTS both highly flexible and efficient. It uses a robust fully implicit THCM (Thermo-Hydro-Chemo-Mechanical)

formulation, allowing us to represent the governing conservation equations for momentum, mass and energy conservation in a generic manner [10]. DARTS utilizes the Operator-Based Linearization (OBL) technique for a generalized and efficient treatment of the different physical terms in the conservation equations [11]. The main advantage of this approach is a simplified implementation of fully coupled fully implicit (FIM) simulation code.

DARTS uses finite-volume approximation on unstructured meshes for the governing PDEs fully coupled with complex thermodynamics of multi-component multiphase systems including equilibrium and kinetic chemistry [12]. To maintain high efficiency for large heterogeneous problems, the linear system is solved using flexible Generalized Minimal Residual Method (GMRES) [13] with a constrained pressure residual (CPR) preconditioner [14]. The Algebraic Multigrid (AMG) method is employed to obtain an approximate solution for the decoupled pressure system in the first preconditioner stage. In the second stage, the classical incomplete Lower-Upper factorization (ILU(0)) preconditioner is applied to the FIM system. DARTS also has advanced inversion capabilities including efficient adjoint gradients implementation [15, 16].

DARTS has been successfully applied for modeling various energy transition applications including hydrocarbon [17, 18], geothermal [19, 20] and CO_2 sequestration [21, 22] problems. The recent implementation of GPU and multithread CPU versions of DARTS makes it a highly efficient simulation platform for energy transition applications [23, 24]. Several extensions include physics-based proxy modeling for compositional problems [25], Adaptive Grid Refinement for geothermal and reactive problems [26] and general-purpose Discrete Fracture Modeling framework [27]. In addition, DARTS has been recently extended for modeling of induced seismicity [10, 28].

2.3 CooresFlow: IFPEN

CooresFlow is a research software developed at IFPEN to simulate multiphase reactive transport in porous media. It is partly composed of two simulators: a 3D reservoir simulator called Geoxim coupled to a 0D/1D geochemical calculator ArximCpp.

Geoxim is a complete reservoir simulator that takes into account the following phenomena: (a) compositional multiphase flow in porous media, with viscous and capillary forces, (b) transport of chemical components by advection, diffusion and dispersion, (c) transfers between the fluids or on the surface of the rock governed by local equilibrium or kinetic reactions to describe thermodynamical and geochemical exchanges, (d) heat convection and thermal conduction, and (e) dynamic modification of the porosity and permeability of the porous medium over time.

Geoxim is written in C++ and is based on the platform ARCANE (a C++-based coding platform [29]) and on ArcGeoSim^{TM}, the IFPEN framework dedicated to the development of geoscientific applications [30]. Thus, Geoxim inherits the high-performance computing (HPC) capabilities of these frameworks such as parallel computing, Local Grid Refinement (LGR) and Adaptive Mesh Refinement (AMR) and other advanced numerical methods.
To solve the non-isothermal compositional multi-phase flow in Geoxim, we use the variable switching formulation introduced by Coats [31] based on natural unknowns (pressure, temperature, phase saturation and species molar fractions). The set of equations is discretized by a fully implicit cell-centered finite volume scheme with a two-point flux discretization. The mobility terms are upwinded with respect to the sign of the phase Darcy flux. Then, the resulting discrete non-linear system is solved using the Newton algorithm and at each iteration, the linear system is solved by an iterative method (PETSC solver like BICGSTAB with ILU0 preconditioner or IFPEN's solvers).

ArximCpp is 0D/1D geochemistry simulator developed in C++ [32] that enables modeling complex fluid-rock interactions. It simulates over time the evolution of mineral proportions and of water composition due to equilibrium and kinetic reactions. ArximCpp integrates several activity models (B-dot, Pitzer, …) and is compatible with many thermodynamic databases (Phreeqc, . . .). Finally, ArximCpp can be used stand-alone or coupled with Geoxim.

These two models are coupled using an iterative splitting method [33]. At each iteration, we first solve the multiphase flow problem with phase equilibrium using Geoxim and in a second step we solve the reactive transport problem using ArximCpp. The multiphase flow model transfers to the reactive transport the following information: the system state (temperature, pressure and volume expansion), the transport properties of water (water saturation, velocities and dispersion tensor) and other information on the water composition. In the other direction, the reactive transport model (ArximCPP) impacts the multiphase flow with the following coupling effects: rock reaction terms, which induce porosity changes, and water reaction terms, which induce a correction of water properties and composition.

In section 3 below the results of CooresFlow were obtained using only Geoxim, except for the last 2D case with extended chemistry (Test 2.2) for which the coupling between Geoxim and ArximCpp was necessary.

2.4 PDELab: Heidelberg University

PDELab is a PDE discretization module based on DUNE [3, 34, 35]. DUNE is a general-purpose finite element framework relying heavily on generic programming techniques to combine both high flexibility and high performance.

PDELab utilizes DUNE to solve a variety of problems including Navier-Stokes problem [36], two-phase flow in porous media [37], and can be also utilized in high-performance codes [38].

We use a structured grid YaspGrid. The problem is discretized with a cell-centered finite volume scheme and the system is solved in a fully-coupled fashion. We use a semi-smooth Newton method with UMFPack solver that solves linear systems exactly. The matrix is calculated by numerical differentiation. The time stepping scheme is backward Euler and the time step size is based on the convergence of the nonlinear solver and the number of its iterations. The maximum time step length is 0.1 days in the 1D cases and 1 day in 2D cases.

We use six primary variables p, S_w, $x_{H_2O,w}$, $x_{CO_2,w}$, $x_{Ca^{2+},w}$, and c_{CaCO_3} (calcite molar concentration, mol/m^3). Besides four mass balance equations for H_2O, CO_2, Ca^{2+}, and $CaCO_3$ we use two complementarity constraints of the form

$$\min\left(1-\sum_{c=1}^{C} x_{c,j},\ S_j\right)=0,\quad j\in\{w,g\}. \tag{1}$$

Complementarity constraints are used to handle the phase disappearance and are equivalent to using primal-dual active set strategy [39]. When one phase disappears, we relax the condition that the sum of molar fractions in that phase is equal to one. This allows molar fractions (that are still tied by fugacity) to attain values that would be otherwise not possible -like initial conditions.

This approach does not work in the extended chemistry scenario. Molar fractions of components that are not present in the gas phase become meaningless when the liquid phase disappears. In simple chemistry cases $x_{Ca^{2+},w}$ remains defined only via its chemical reaction, but in the extended chemistry case there are several such components and the matrix is singular.

2.5 MIN3P : EOAS-UBC

MIN3P is a multicomponent reactive transport code, specifically designed for simulating flow and reactive transport processes in variably saturated media. Previous applications include the simulation of the generation and attenuation of acid rock drainage in mine tailings and waste rock [40, 41], biogeochemical processes in forested soils [42], natural attenuation of petroleum hydrocarbon spills in shallow unconfined aquifers [43], carbon sequestration in ultramafic mine waste [44], and gas migration in the context of natural gas leakage from energy wells [45]. To provide flexibility, MIN3P allows consideration of a wide range of biogeochemical reaction networks including hydrolysis, aqueous complexation, ion exchange, surface complexation, gas partitioning, redox equilibria and mineral dissolution-precipitation through a database. MIN3P also includes a generalized framework for kinetically controlled reactions to model a wide range of intra-aqueous and heterogeneous rate-controlled processes [40, 42]. The solution algorithm of the original code relies on the solution of groundwater flow, sequentially followed by the solution of the reactive transport problem [46, 47]. For reactive transport, the code uses the global implicit method, applying the direct substitution approach (DSA) [40]. Spatial discretization is performed based on the finite volume method for structured and unstructured grids [48] and the overall solver uses a fully implicit and adaptive time-stepping strategy to minimize CPU time requirements [42, 46]. The software is developed in Fortran 90.

The code has recently been extended to tackle coupled problems involving multiphase flow and biogeochemical reactions through a compositional formulation. In this approach, water is considered as a chemical component and its mass conservation equation is included directly in the reactive transport framework. A separate solution of the groundwater flow problem is no longer required. The method is based on the traditional reactive transport equations (solving for the mass balance of total component concentrations) but utilizes molar fractions, liquid phase pressure, and liquid phase saturation as primary unknowns. The overall system is solved by a fully implicit scheme using a Newton semi-smooth method to handle the local appearance/disappearance of a gas phase without a discontinuous switch of primary variables [49]. The model has been validated for several coupled solute-solvent systems and results have been compared to the sequential groundwater flow and reactive transport solver [46].

2.6 GEOS: TTE-LLNL-SU

GEOS [50] is an open-source, multiphysics simulator written cooperatively by Lawrence Livermore National Laboratory, Stanford University, and TotalEnergies to support the development of greenhouse gas mitigation technologies such as geologic carbon storage and other subsurface energy systems. The software is based on a portable C++ computational platform targeting massively parallel CPU/GPU architectures and provides access to scalable linear solvers and preconditioners from the Hypre, Trilinos, and PETSc packages. GEOS relies on a finite volume (for flow) – finite element (for mechanics) scheme to simulate thermal multiphase flow and mechanics with faults and fractures in a fully coupled fashion. Thanks to a flexible mesh infrastructure and advanced numerical schemes [51, 52], these simulations can be performed on complex unstructured grids that conform to the geometrical features of the porous medium.

Table 1 Definition of different problems

Name of the problems	Dimension	Chemistry			Gravity
		Base		Extended	
		Kinetic	Equilibrium		
1.1	1D	✓			
1.2	1D		✓		
2.1 no grav	2D	✓			no
2.1 grav	2D	✓			yes
2.2	2D			✓	yes

Recently, the GEOS team has been collaborating with TU Delft to implement reactive transport modeling in flow-only simulations using the Operator-Based Linearization (OBL) strategy for the residual and Jacobian assembly [11, 17]. In this approach, the discretized equations are split into space- and state-dependent terms. The state-dependent terms (e.g. the convective flux) are referred to as operators. Instead of calculating the operators precisely for the entire state (i.e., parameter) space, a discretization in the state space is applied. The operator values are calculated only for these supporting points. To obtain the values and derivatives of the operators for the entire state space, a multilinear interpolation is applied. The interpolant required to interpolate the operator's value in a particular hypercube is the partial derivative. This implies simple, exact, and flexible Jacobian assembly for the nonlinear solution procedure since it is only necessary to know the operator value at the supporting points.

The implementation of OBL in GEOS is preliminary. In particular, the operator values must currently be calculated at all supporting points as a pre-processing step. This imposes a limit on the number of supporting points that can be used in the simulations, which in turn might negatively impact the accuracy of the results in some cases. This is for instance the case in Section 3.3 of benchmark suite.

Newton's method with damping is used to solve the nonlinear systems at each time step and update all the degrees of freedom (pressure and component fractions) fully implicitly. The linear systems are solved with GMRES accelerated by a block-triangular preconditioner implemented in the Multi-Grid Reduction framework [53, 54] provided by Hypre. Although the reactive transport feature of GEOS is tested for the first time in this benchmark, the other GEOS capabilities have been presented in previous publications [55–59].

3 Comparison and discussion of the results

In this section, we discuss the various test cases, and compare the results of the different codes and their numerical performance. We note that, for the sake of conciseness, we only show a subset of all the results that were computed by the participants. In particular, we have left out all discussions of Test case 1.2 (1D simple chemistry with equilibrium), as both the physical results and the performance of the codes were very similar to test case 1.1. The complete set of results can be found in Online Resource 1.

Table 1 shows a summary of the features of the different cases (refer to the companion paper [1] for full details), while Table 2 shows which test cases were solved by each of the participating groups. We note that all codes used a finite volume method. Also, all codes (with the exception of CooresFlow for Test case 2.2, where a splitting method is used) used a fully implicit formulation where the non-linear system occurring at each time step is solved by some variant of Newton's method, possibly including a variable switching mechanism. Finally, we add that the test cases for GEOS were run with OpenMP parallelization with 36 threads. The times reported below are elapsed times.

Table 2 Description of simulators participation to the benchmark, computer architecture used

Code	Institution	Participation in problems	Architecture
DuMu^X	UPPA-Inria	1.1, 1.2, 2.1 no grav, 2.1 grav, 2.2	Intel i7-8565U @1.8 GHz
DARTS	TU-DELFT	1.1, 1.2, 2.1 no grav, 2.1 grav	Intel i7-6700HQ @2.6 GHz
CooresFlow	IFPEN	1.1, 1.2, 2.1 no grav, 2.1 grav, 2.2	Intel Xeon E5-1620 v3 @3.5 GHz
MIN3P	UBC	1.1, 1.2, 2.1 no grav	Intel Xeon E5-2680 v2 @2.8 GHz
PDELab	Uni. Heidelberg	1.1, 1.2, 2.1 no grav, 2.1 grav	Intel Xeon E5-2698 v3 @2.3 GHz
GEOS	TTE-LLNL-SU	1.1, 2.1 no grav, 2.1 grav	Intel Xeon E5-2695 v4 @2.1 GHz

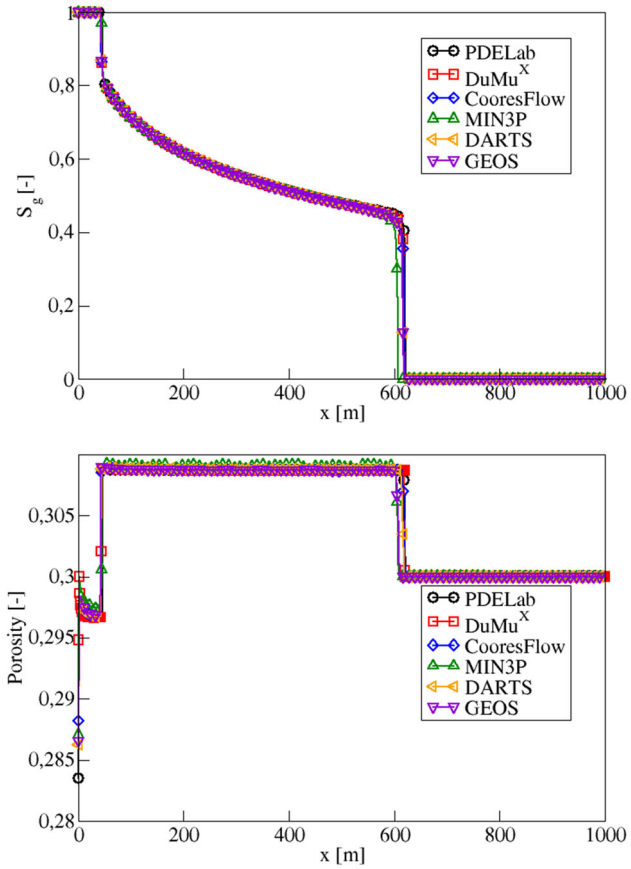

Fig. 1 Comparison of gas saturation (top) and porosity (bottom) at $t = 1000$ days for the Test 1.1

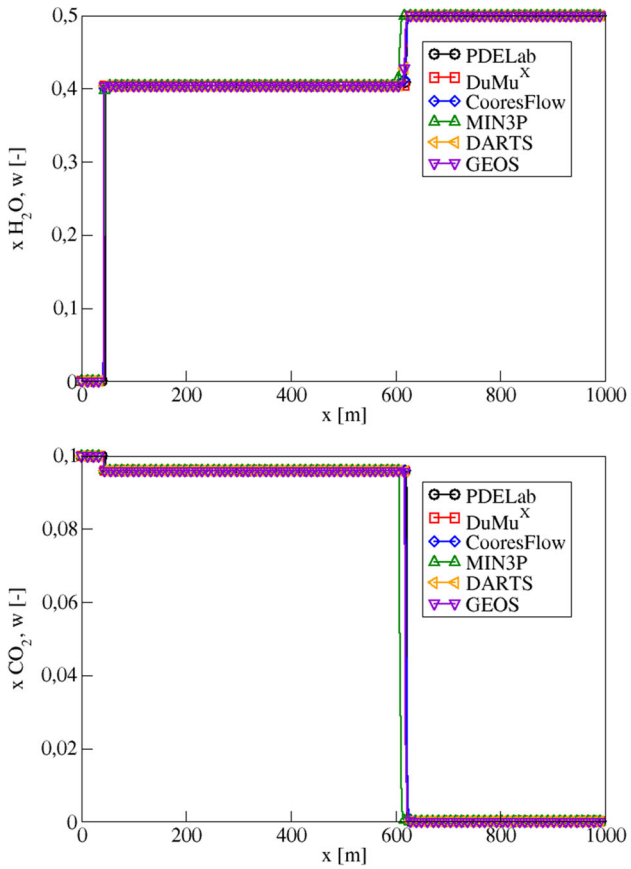

Fig. 2 Comparison of $x_{\mathrm{H_2O},w}$ (top) and $x_{\mathrm{CO_2},w}$ (bottom) at $t = 1000$ days for the Test 1.1

3.1 Test 1.1

The first test case uses a 1D geometry with the basic chemical system in kinetic mode. It was solved by all participants. This test represents the results of the simulation involving two phenomena: two-phase compositional flow and transport with chemical dissolution and precipitations in an aquifer experiencing CO_2 injections. The graphs shown in Figs. 1 and 2 compare the results obtained by the participants at the final time $t = 1000$ days as a function of space. We show in Fig. 1 the gas saturation and the porosity and on Fig. 2 the molar fractions of CO_2 and H_2O in the liquid phase. The displacement process is characterized by trailing and leading shocks clearly observed at the top of Fig. 1. These shocks correspond to compositional transport along a fixed tie-line (due to the fixed K-values) and follow closely the theory of gas injection [60]. These two shocks confine a two-phase region where CO_2 and water co-exist at thermodynamic equilibrium.

Due to the presence of CO_2, the rock is dissolved up to a certain limit, which explains the increase in porosity in the two-phase region, see bottom of Fig. 1. The simulation results are consistent with the proposed geochemical model where calcite precipitation and dissolution is only a function of the Ca^{2+} and CO_3^{2-} molar fractions. The injection of CO_2 gas decreases the ions' molar fraction, which induces mineral dissolution. Moreover, liquid phase vaporization causes calcite precipitation in the single-phase gas region located before the trailing shock. Here, ions dissolved in water precipitate to form calcite, which reduces the porosity below the initial values. Due to the loss of the water phase into the dry gas stream near the inlet, evaporation occurs, leading to the precipitation of calcite and porosity reduction.

Figures 3 and 4 compare the gas saturation, porosity, pressure and H_2O molar fraction obtained by the participants, now as a function of time at the point $x = 25$ m. For this test case, all the codes have performed in a similar way, though the precise location of the front shows some differences, in particular as a function of time in Figs. 3 and 4. One can see some oscillations in the pressure for all the codes in Fig. 4. This phenomenon can be explained by the original design of the benchmark. The flow system is close to incompressible, which yields an almost constant velocity in the entire domain. However, the dissolution and precipitation process is changing porosity and permeability following displacement shocks. This process is strongly localized in

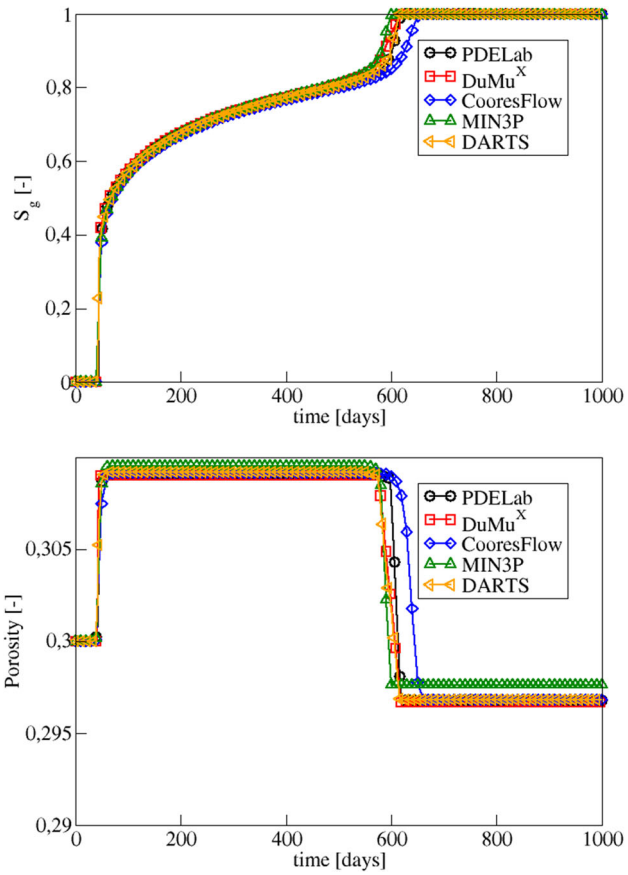

Fig. 3 Comparison of gas saturation (top) and porosity (bottom) at $x = 25$ m for the Test 1.1

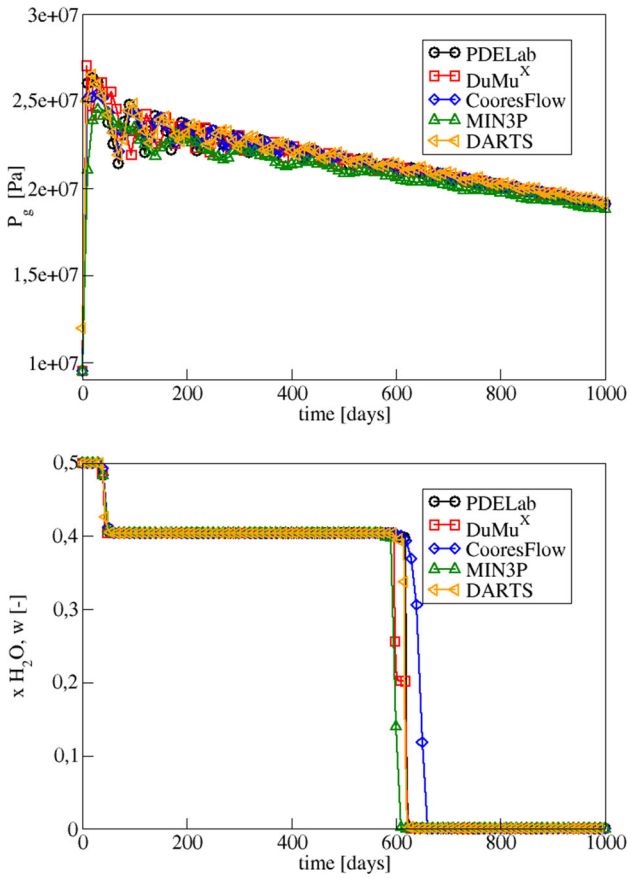

Fig. 4 Comparison of pressure (top) and H_2O molar fraction (bottom) at $x = 25$ m for the Test 1.1

the discretized numerical problem and causes block-by-block porosity/permeability adjustments. These changes require a correction in pressure to maintain an almost constant velocity of the low-compressible system, which explains pressure oscillations.

3.1.1 Grid convergence analysis

In order to assess the accuracy of the results, and also their sensitivity to the grid resolution, we have performed a numerical convergence study. Since we saw in the previous Section that all codes agreed for this problem, the convergence study was only performed with DuMu^X.

Numerical convergence in space We first assess the spatial accuracy, using a number of elements varying from 100 to 2000. The top part of Fig. 5 compares the gas saturation profiles computed with the various resolutions using a maximal time step equal to 0.1 day. It shows that using on the order of 1000 elements is both necessary and sufficient to obtain a good accuracy. Additionally, the bottom part of Fig. 5 shows the convergence rate for the various computed quantities as the mesh is refined (using the solution on the finest grid as the reference solution). A convergence rate close to 0.7 is visible, confirming that the solution is converging as the mesh size decreases.

Numerical convergence in time In a second step, the number of elements in space is kept fixed at 1000, while the maximal time step is decreased. Figure 6 compares the gas saturation computed for three different time steps. It can be observed that, as long as the maximum time step remains between 0.1 days and 1 day, its value has no influence on the shape and the position of the saturation front.

3.1.2 Performance of the numerical methods

Table 3 shows, for each participant, the total number of time steps taken by the code, the average number of non-linear iterations per time-step, the average number of linear iteration per Newton iterations and the CPU time. The number of failed attempts for each quantity is shown between parentheses. It can be seen that the performance in terms of the average number of Newton iterations per time step and of an average number of linear iterations per Newton iteration are comparable, even though the participants used very differ-

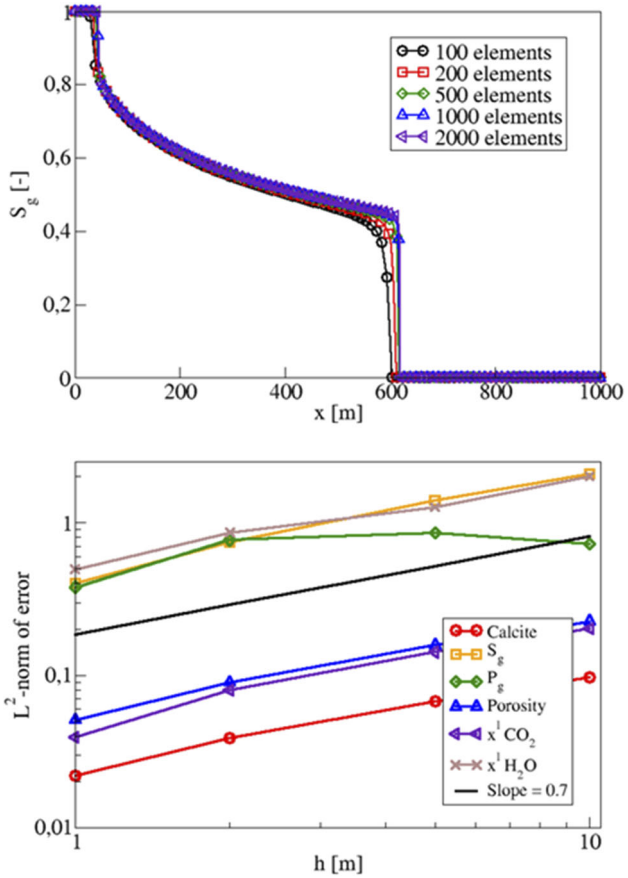

Fig. 5 Comparison of saturation at $t = 1000$ days using different meshes (top). Convergence analysis in L^2-norm (bottom)

ent formulations. The difference in the number of time steps taken by each code is a reflection of the maximum time step imposed, which is either 0.1 day or 1 day. In both cases, the maximum time step was reached very quickly. The largest difference in performance is in the CPU time, and this may

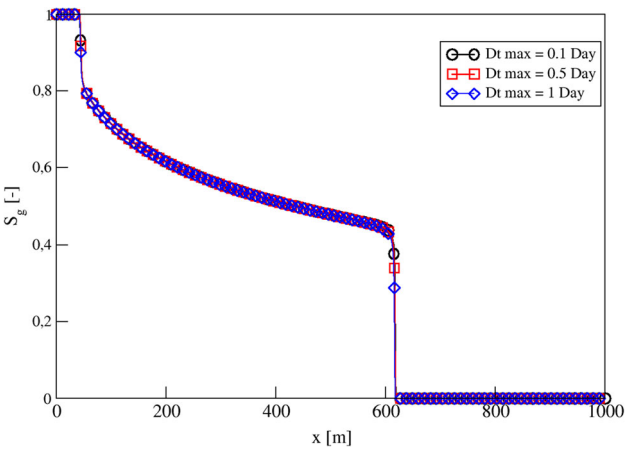

Fig. 6 Comparison of gas saturation at $t = 1000$ days using different maximal time steps (mesh composed of 1000 elements)

be explained by several factors: first of all, the number of time steps has a direct impact on the CPU time, then various algorithmic choices such as convergence tolerance for the iterative processes may also have an impact, the implementation efficiency may vary across codes, and the simulations were run on different processors from different generations, with different clock rates, and possibly on several cores. This observation is valid for all the test cases, and will not be repeated.

3.2 Test 2.1 without gravity

This test case, as well as the following ones, uses a 2D geometry while retaining the basic chemical system. In this simulation, the effects of gravity are neglected. This test case was solved by all participants. In a preliminary step, we investigated the sensitivity of the results to the spatial grid resolution. Figure 16 in the appendix represents the gas saturation computed by DARTS for several meshes composed of 60×24, 120×48, 240×96 and 480×192 elements. Based on the results in Fig. 16, we believe that the mesh composed of 120×48 elements is fine enough for the results to be considered sufficiently accurate to be suitable for the code intercomparison. Therefore, this mesh has been used for all the numerical results presented for Test 2.1 with and without gravity as well as for Test 2.2.

In order to make it easier to interpret the comparison results that are given at the final time, we first present two snapshots of the solution at earlier times. The results shown were computed with DuMu^X. Figure 7 represents the gas saturation at $t = 200$ days and $t = 400$ days. It can be seen that the injected gas is first completely dissolved in water and once the maximum solubility is reached, the gas phase appears. The gas saturation front moves preferentially to the right because water injection in the upper half of the left boundary prevents it from entering the upper half of the domain. The arrival of the gas front in the central part with higher permeability creates a second, faster, front (see the top of Fig. 7). We thus observe the coexistence of two fronts with different velocities. The fastest front spreads as it leaves the most permeable area (see bottom of Fig. 7).

Figures 8 and 9 compare respectively the gas saturation and the porosity obtained by the six codes at the final time $t = 1000$ days. The results are fairly close, with some differences that can be attributed to the way the boundary conditions on the right are specified. The current multiphase implementation in MIN3P does not permit the gas phase saturation to increase on the right boundary, which leads to a gas phase build-up on the right side of the domain towards the end of the simulation. We can see in Fig. 8 that both fronts observed in Fig. 7 are still visible and they will end up merging at the outlet of the domain. The injection of

Table 3 Numerical performance of the codes for Test 1.1. TS: number of time steps, NI: Average number of nonlinear iterations per time step, LI / NI: average number of linear iterations per Newton iteration, CPU: elapsed time

Code team	TS (failed)		NI (failed)		LI / NI (failed)		CPU (sec)
DuMu^X	13092	(1251)	2.98	(1.9)	1.63	(8)	564
DARTS	1009	(0)	2.39	(0)	2.99	(0)	15
CooresFlow	1000	(0)	4.92	(0)		not available	259
PDELab	10000	(0)	3.01	(0)		exact solver	1006
MIN3P	3125	(200)	19.01	(1.31)	1.0	(0)	1045
GEOS	1010	(0)	2.38	(0)	1.08	(0)	75

pure water across the upper half of the left border flushes out Ca^{2+} and CO_3^{2-} ions, creating a calcite dissolution front. This front ends up being completely dissolved by the end of the simulation and the porosity tends towards 1 as shown in Fig. 9.

Figure 10 compares the same quantities along the horizontal line $y = 50$ m. We can observe on the left image of Fig. 10 that, close to the injection, the liquid phase disappears. As demonstrated by the one-dimensional simulation, there is a direct link between saturation evolution and porosity behavior. In the fully gas-saturated region near the injection, the porosity reaches minimal values due to calcite precipitation. The low value of saturation close to $x = 400$ m illustrates the presence of the two fronts and locally increases the porosity due to the calcite dissolution, creating a very noticeable peak in porosity (right image of Fig. 10).

The performance of the codes for this test case is shown in Table 4, with the same entries as in Table 3. The behavior of the different codes with respect to the iterative methods is comparable. The number of time steps is different, again because of the choice of the maximal allowed time step.

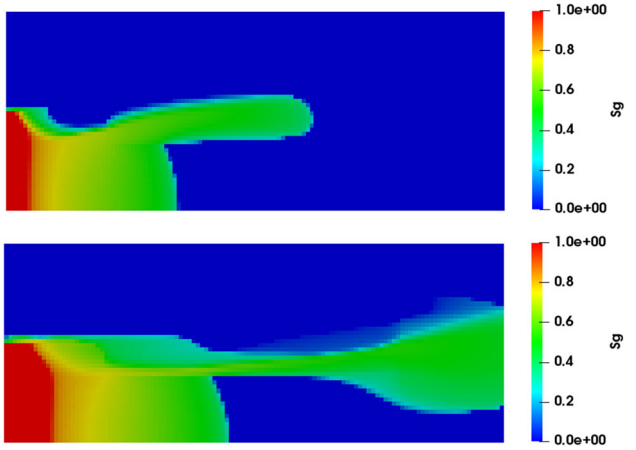

Fig. 7 Gas saturation at $t = 200$ days (top) and $t = 400$ days (bottom) for the Test 2.1 without gravity

3.3 Test 2.1 with gravity

This test case is identical to Test case 2.1, with the difference that gravity effects are now included. Five teams attempted this test case (all but MIN3P).

Here again, we first show snapshots of the solution at earlier times, to ease the interpretation of the comparisons in Figs. 12, 13, and 14. Figure 11 represents the evolution of the gas saturation at two instants (computed with DuMu^X). As expected, the behavior of the flow is significantly different from what was observed in the case without gravity. Gravity makes the gas rise to the top of the domain before it starts moving to the right. Its arrival in the high permeability zone creates a preferential path (see top of Fig. 11). Porosity is not presented but its evolution is very close to the one of case 2.1 without gravity depicted in Fig. 9. Calcite is completely dissolved close to the pure water injection. As a consequence, the porosity and permeability are strongly enhanced and the gas front ends up reaching the top left part (see bottom of Fig. 11). Despite its higher permeability, the area in the center of the domain is almost not reached by the gas due to its buoyancy.

The results at $t = 1000$ days obtained by the different codes are compared in Figs. 12, 13 and 14. The results are in good qualitative agreement. The main difference between simulations concerns the upper left zone, close to the pure water injection. For certain codes, the low values for gas saturation lead to the absence of dissolved CO_2. It can also be noted that all the codes succeeded in capturing the localized region without gas in the upper part, even if its shape and size differ slightly from one code to another.

For this test case, GEOS exhibits noticeable differences with the other codes. This is due to the fact that the Operator-Based Linearization [11] implementation in GEOS is preliminary and currently requires the operator values to be computed at all supporting points in a pre-processing step. This is memory-demanding and limits the number of available supporting points, which undermines accuracy. To overcome this limitation and allow for more supporting points, the GEOS developers plan to implement an adaptive,

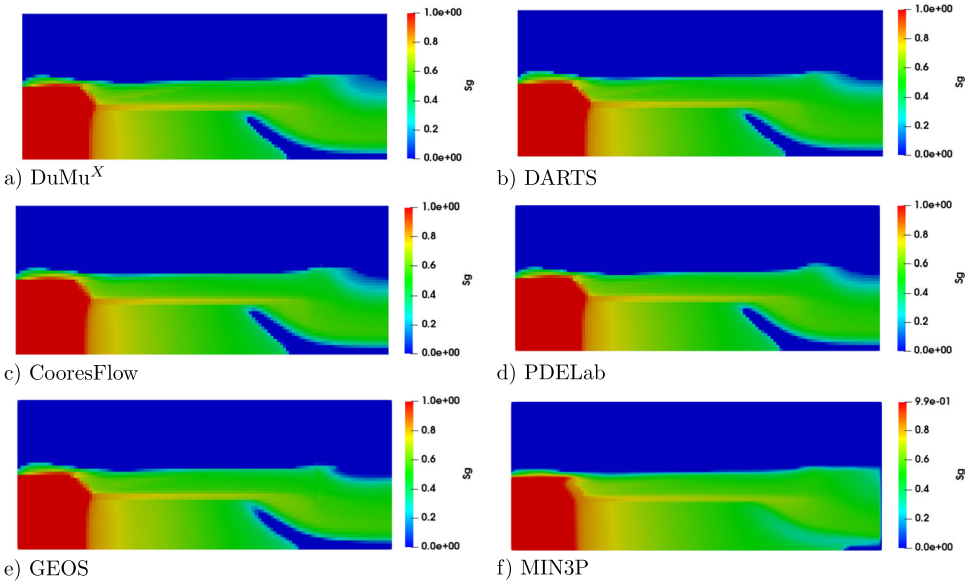

Fig. 8 Comparison of S_g at $t = 1000$ days for the Test 2.1 without gravity

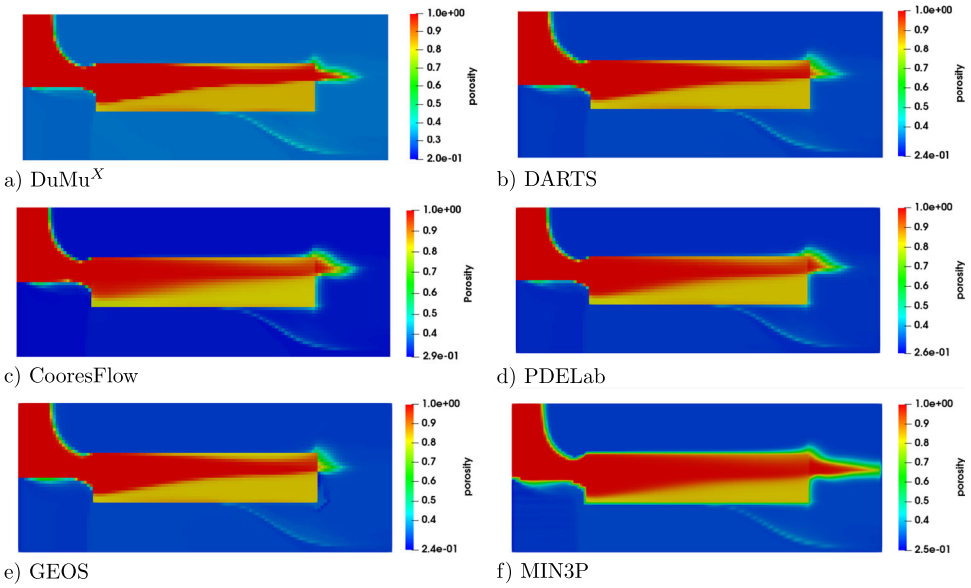

Fig. 9 Comparison of ϕ at $t = 1000$ days for the Test 2.1 without gravity

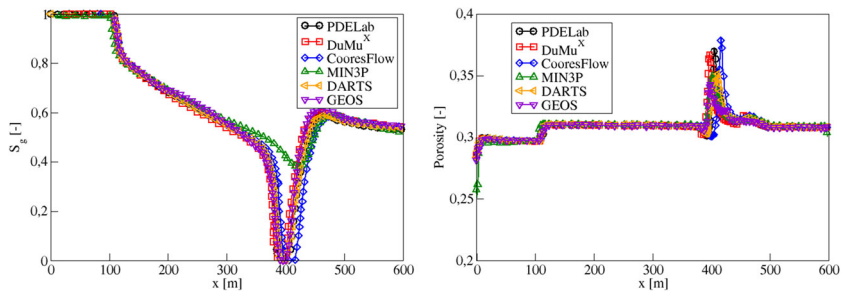

Fig. 10 Comparison of gas saturation (left) and porosity (right) at $t = 1000$ days on the horizontal line $y = 50$ m for the Test 2.1 without gravity

Table 4 Numerical performance of the codes for Test case 2.1 without gravity. See legend of Table 3 for the meaning of the abbreviations

Code team	TS (failed)		NI (failed)		LI / NI (failed)		CPU (sec)
DuMu^X	11833	(782)	4.11	(18)	7.19	(0)	8755
DARTS	1009	(0)	2.36	(0)	9.76	(0)	449
CooresFlow	2008	(0)	2.46	(0)		not available	2937
PDELab	1000	(0)	4.73	(0)		exact solver	3891
MIN3P	14574	(1386)	12.24	(1.29)	112		106184
GEOS	1053	(0)	3.35	(0)	28.5		925

on-the-fly computation of the operator values as the simulation progresses.

The performances of the codes for this test case are shown in Table 5, with the same entries as in Table 3. The observations are similar. We note in particular that the numbers for both the Newton and the linear iterations remain fairly low. In this case, the number of time steps is more varied, as some codes experience failed steps. This also explains the larger number of Newton failures, even though the time-step management strategies are successful at preventing too many failures.

3.4 Test 2.2

This test case is the only one that features the "extended" chemical system. We remind the reader that this test case also takes gravity into account. It has only been attempted by two codes: DuMu^X and CooresFlow. The results for several quantities (gas saturation, molar fraction of dissolved CO_2, pH and molar fraction of dissolved Ca^{2+} ion) are shown in Fig. 15.

We remind the reader that not only is the chemical system more complex (with additional aqueous reactions at equilibrium), but also that the dissolution constant for calcite is more

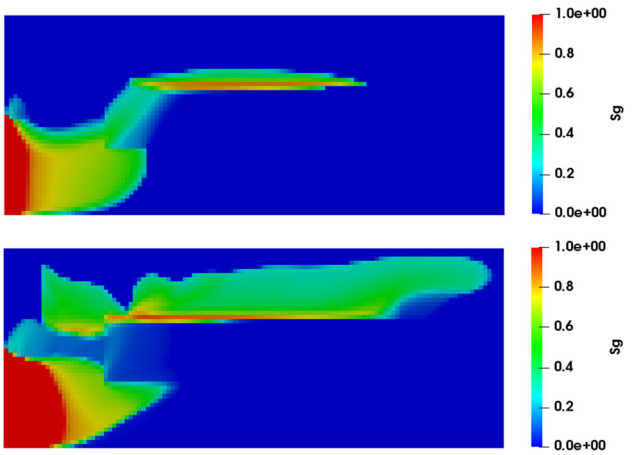

Fig. 11 Gas saturation at $t = 200$ days (top) and $t = 600$ days (bottom) for the Test 2.1 with gravity (computed with DuMu^X)

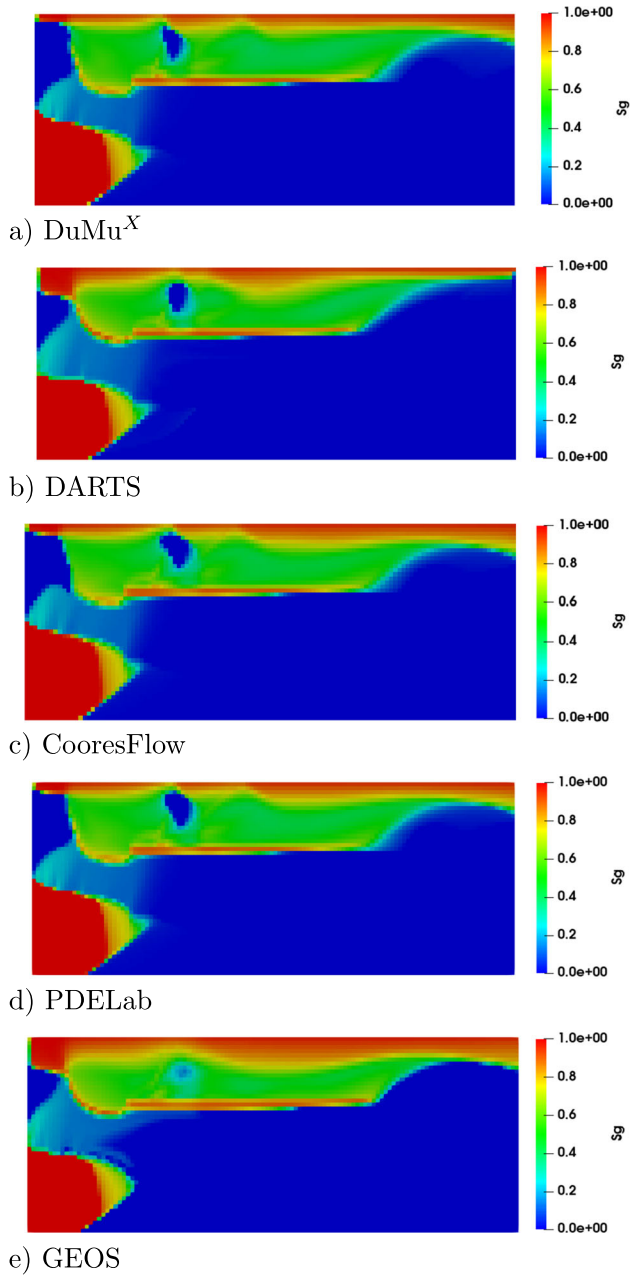

Fig. 12 Comparison of S_g at $t = 1000$ days for the Test 2.1 with gravity

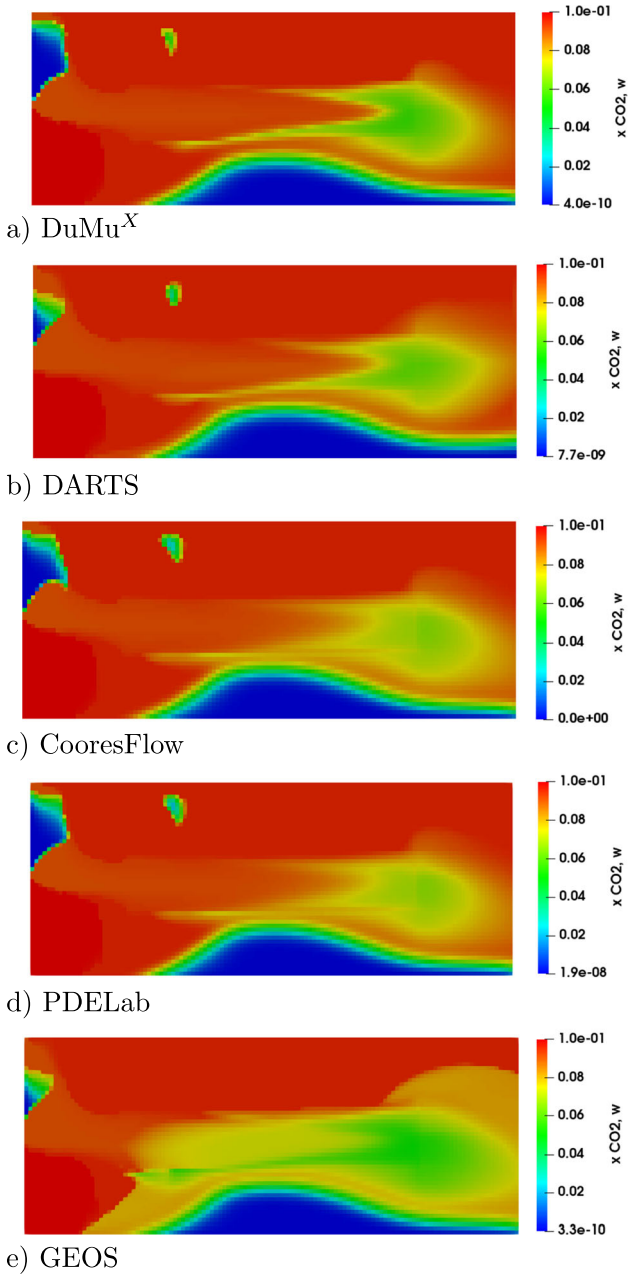

Fig. 13 Comparison of $x_{CO_2,w}$ at $t = 1000$ days for the Test 2.1 with gravity

realistic and about five times smaller than in the previous test cases, thus leading to much less calcite dissolution. This remark helps explain the shape of the gas saturation profile in the top images of Fig. 15 (compare with Fig. 12). While the initial evolution for the gas is the same as in test case 2.1 with gravity, the fact that calcite has almost not dissolved over the duration of the simulation means that no path towards the upper left part of the domain was created and that the gas has only migrated towards the upper right. For the same reason, there is no liquid CO_2 in the upper left part of the domain because the gas has not reached this area and thus has not dissolved. For the two bottom rows in Fig. 15, the pure water injected from the top left area has displaced the ions from this area so that the concentration in H^+ and Ca^{2+} ions is small, and the pH is high. On the other hand, we note that the values for the ions in the bottom left part of the images have no real physical meaning as this part has no liquid phase.

The two codes are in at least qualitative agreement for this test case.

The performance of the codes for this test case is shown in Table 6, with the same entries as in Table 3. We note that in Table 6, the number of Newton iterations for CooresFlow corresponds only to the number of iterations performed for solving the multiphase flow problem by Geoxim. However, at each time step, the nonlinear reactive transport problem is also solved by an iterative Newton method in ArximCpp. However the number of Newton iterations is not directly accessible in ArximCpp, so it is not shown in Table 6.

4 Discussion and conclusions

We can now draw some conclusions regarding the benchmark and also present possible future research directions. The present discussion takes some inspiration from the MoMaS benchmark synthesis paper [61].

As was our hope, the benchmark was a useful tool to help compare several codes on a relevant (albeit not realistic) situation. The fact that we had chosen fictitious data for the benchmark, both for the physical parameters and for the chemical system, has the obvious drawback that some

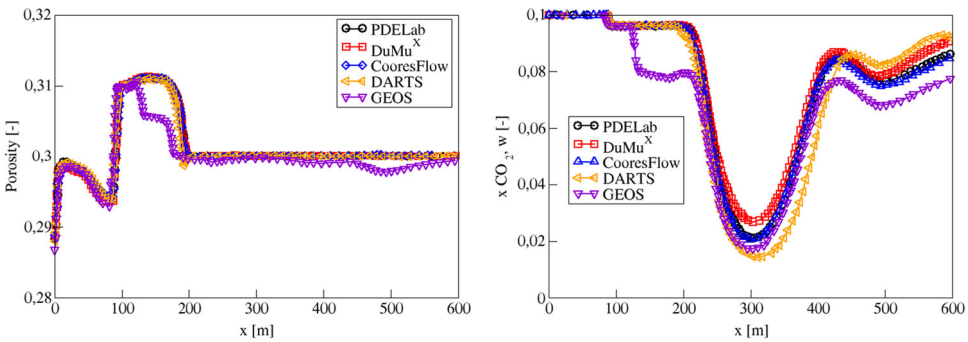

Fig. 14 Comparison of porosity (left) and CO_2 molar concentration (right) at $t = 1000$ days on horizontal line $y = 50$ m for the Test 2.1 with gravity

Table 5 Numerical performance of the codes for Test case 2.1 with gravity. See legend of Table 3 for the meaning of the abbreviations

Code team	TS (failed)		NI (failed)		LI / NI (failed)		CPU (sec)
DuMu^X	10767	(310)	3.53	(10.54)	9.62	(3.62)	8609
DARTS	1019	(18)	2.46	(9.9)	12.57	(13.6)	589
PDELab	2376	(38)	4.73	(19.6)	exact solver		9449
CooresFlow	3996	(742)	3.84	(0)	not available		7592
GEOS	1152	(52)	3.28	(0.45)	38.14	(6.54)	1177

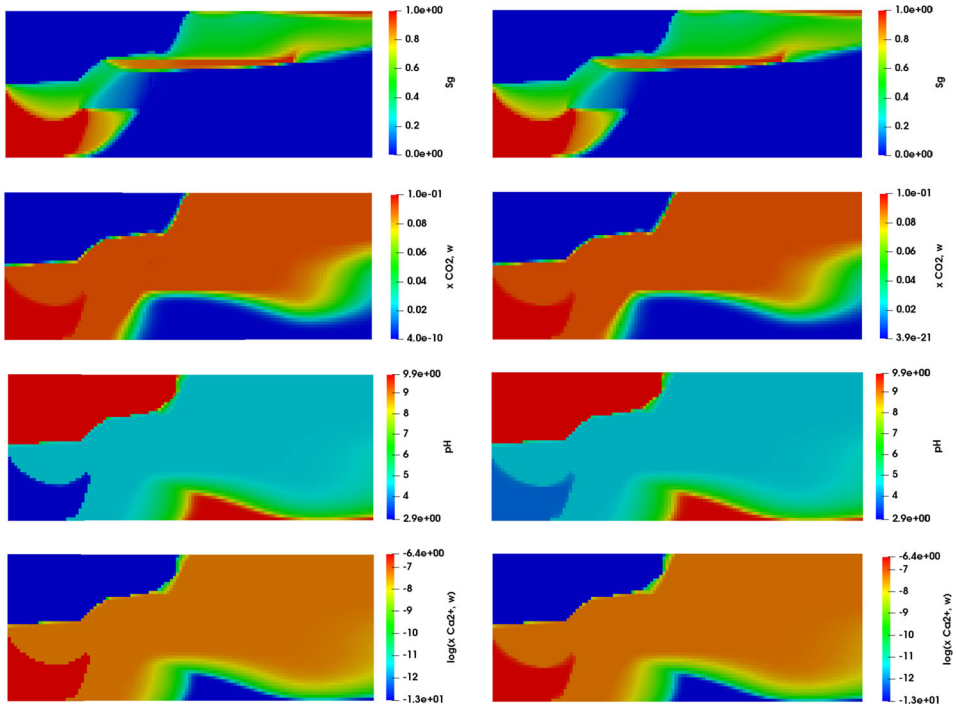

a) DuMu^X b) CooresFlow

Fig. 15 Comparison at $t = 1000$ days for the Test 2.2 with gravity

Table 6 Numerical performance of the codes for Test case 2.2. See legend of Table 3 for the meaning of the abbreviations

Code team	TS (failed)		NI (failed)		LI / NI (failed)		CPU (sec)
DuMu^X	17571	(2937)	3.45	(1.71)	8.37	(13.04)	66124
CooresFlow	2008	(0)	4.1	(0)	not available		10224

conclusions may not be fully applicable to more realistic situations. However, based on this and previous experience, we still believe that the conclusions reached in this paper have a more general value. Additionally, having a fully specified set of parameters for, say the equations of state and the relative permeability, enabled us to focus purely on numerical issues. Any difference in the results can be attributed to either the nonlinear formulation or the discretization, and not to a different choice of parameters.

The fact that the results from all methods were comparable, even though there still remained some noticeable differences, gives increased confidence in the validity of the model formulation and of the results. We can also add that most groups needed to add some specific modifications to their codes to be able to run the various test cases, thus giving them some extra functionality and performing a demanding validation at the same time.

Some teams have been able to study the grid sensitivity (both in 1D, see Section 3.1.1 and in 2D, see Appendix A). It appears that the results are quite sensitive to the resolution used which is a known issue in compositional simulation [62, 63].

The question of validating the results for such a complicated physical model is a legitimate one[1]. While we have no complete answer for a setup like the one presented here, the facts that the codes agreed in principle, and that grid convergence was reached, give us reasons to believe the results presented are meaningful.

We cannot avoid mentioning the perennial issues of "splitting vs fully implicit". We just note that for almost all the presented results, all codes used a fully implicit approach, as detailed in the relevant subsections of Section 2. This may be an indication that both the software and the hardware have now matured to the point that the fully implicit approach becomes the default one. The exception (CooresFlow with ArximCpp for the last test case) shows first of all that this approach is valid if implemented carefully, and second that it may still be required for coupling two existing codes. The fully implicit approach included the (quite simplified) chemical equations in the flow model. However, coupling with a genuine geochemistry code may only be feasible with a splitting (or more properly, fixed point) approach.

Several directions for further research emerge after this work:

- Dealing with a more complete chemical system was perhaps the most glaring shortcoming of the present work. Given the difficulties encountered with this simplified setting, coupling a full compositional code with a geochemical code will certainly present formidable challenges. Finding the most appropriate formulation for the coupled problem is far from settled, and the coupling algorithm will also require some further work, as discussed above.
- Most codes participating in this benchmark exercise were based on extensions of established multiphase flow or compositional simulators, while MIN3P is a multicomponent reactive transport code expanded to account for multiphase flow processes. The results suggest that it may be challenging to match the performance of the multiphase flow codes by expanding multicomponent reactive transport codes; however, on the upside geochemical capabilities are readily available in existing multicomponent reactive transport codes.
- Including other physical phenomena, such as a non-isothermal model or mechanical effects, may be important for realistic simulations of underground CO_2 storage.
- A different direction would be to set up a more realistic geometry, representative of existing geological reservoirs. This requires a 3D geometry, would entail a much larger computational problem and would necessitate the use of highly parallel codes.

[1] The issue arose from a question asked by S. Pop at the second SITRAM workshop

Supplementary Information The online version contains supplementary material available at https://doi.org/10.1007/s10596-024-10269-y.

Funding The work of E. Ahusborde, B. Amaziane and M. El Ossmani has been partly supported by the Carnot ISIFoR Institute, and "la Région Nouvelle-Aquitaine", France. These supports are gratefully acknowledged. A. Socié and D. Su were supported by the Government of Canada through a Natural Sciences and Engineering Research Council of Canada - Strategic Partnership Grant for Networks (NETGP 479708-15). F. Hamon was supported by TotalEnergies through the FC-Maelstrom project.

Data availability The results obtained by the participants in this benchmark study can be found on the website: https://github.com/eahusbor/Reactive-Multiphase-Benchmark. Furthermore, the DARTS model scripts needed to reproduce the results for the test cases using the basic chemical model can be found at https://gitlab.com/open-darts/darts-models.

Declarations

Competing interests The authors have no competing interests to declare that are relevant to the content of this article.

Appendix A

Convergence analysis for Test 2.1

In this section, we briefly investigate the sensitivity of the reported results with respect to the mesh discretization for

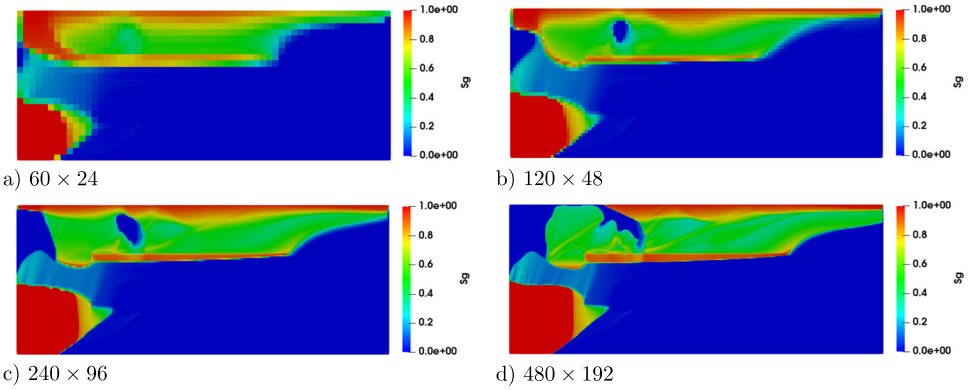

Fig. 16 Comparison of gas saturation at $t = 1000$ days for the Test 2.1 with gravity using different meshes (computed with DARTS)

the 2D Test case 2.1 (section 3.1.1 contains a similar study for the 1D Test 1.1). The computations were carried out with the code DARTS, but the authors believe that the same conclusions would have been reached with the other codes.

Figure 16 represents the gas saturation computed by DARTS for several meshes composed of 60×24, 120×48, 240×96 and 480×192 elements.

One can see that the results obtained on the coarsest grid (Fig. 16-a) lack several features that can be seen at finer resolutions. Differences can still be seen on all four meshes; however, the main qualitative features have mainly stabilized from mesh (b)-onwards. Mesh (b) (with 120×48 elements) was chosen as an acceptable compromise between sufficient accuracy and a reasonable computation time for the numerical experiments.

References

1. de Hoop, S., Voskov, D., Ahusborde, E., Amaziane, B., Kern, M.: A benchmark study on reactive two-phase flow in porous media: Part I - model description. Comput. Geosci. (2024). https://doi.org/10.1007/s10596-024-10268-z
2. Koch, T., Gläser, D., Weishaupt, K., Ackermann, S., Beck, M., Becker, B., Burbulla, S., Class, H., Coltman, E., Emmert, S., Fetzer, T., Grüninger, C., Heck, K., Hommel, J., Kurz, T., Lipp, M., Mohammadi, F., Scherrer, S., Schneider, M., Seitz, G., Stadler, L., Utz, M., Weinhardt, F., Flemisch, B.: DuMu^X 3 - an open-source simulator for solving flow and transport problems in porous media with a focus on model coupling. Comput. Math. Appl. **81**, 423–443 (2021). https://doi.org/10.1016/j.camwa.2020.02.012
3. Bastian, P., Blatt, M., Dedner, A., Dreier, N.A., Engwer, C., Fritze, R., Gräser, C., Grüninger, C., Kempf, D., Klöfkorn, R., Ohlberger, M., Sander, O.: The DUNE framework: Basic concepts and recent developments. Comput. Math. Appl. **81**, 75–112 (2021). https://doi.org/10.1016/j.camwa.2020.06.007
4. Ahusborde, E., Kern, M., Vostrikov, V.: Numerical simulation of two-phase multicomponent flow with reactive transport in porous media: application to geological sequestration of CO_2. ESAIM: Proc. **50**, 21–39 (2015). https://doi.org/10.1051/proc/201550002
5. Ahusborde, E., El Ossmani, M.: A sequential approach for numerical simulation of two-phase multicomponent flow with reactive transport in porous media. Math. Comput. Simul. **137**, 71–89 (2017). https://doi.org/10.1016/j.matcom.2016.11.007
6. Ahusborde, E., Amaziane, B., El Ossmani, M.: Improvement of numerical approximation of coupled two-phase multicomponent flow with reactive geochemical transport in porous media. Oil & Gas Science and Technology - Rev. IFP Energies nouvelles **73** (2018). https://doi.org/10.2516/ogst/2018033
7. Ahusborde, E., Amaziane, B., El Ossmani, M., Id Moulay, M.: Numerical modeling and simulation of fully coupled processes of reactive multiphase flow in porous media. J. Math. Study **52**, 359–377 (2019). https://doi.org/10.4208/jms.v52n4.19.01
8. Ahusborde, E., Amaziane, B., Id Moulay, M.: High performance computing of 3D reactive multiphase flow in porous media: Application to geological storage of CO_2. Comput. Geosci. **25**, 2131–2147 (2021). https://doi.org/10.1007/s10596-021-10082-x
9. Voskov, D., Saifullin, I., Wapperom, M., Tian, X., Palha, A., Orozco, L., Novikov, A.: open Delft Advanced Research Terra Simulator (open-DARTS). https://doi.org/10.5281/zenodo.8116928
10. Novikov, A., Voskov, D., Khait, M., Hajibeygi, H., Jansen, J.D.: A scalable collocated finite volume scheme for simulation of induced fault slip. J. Comput. Phys. **469** (2022). https://doi.org/10.1016/j.jcp.2022.111598
11. Voskov, D.V.: Operator-based linearization approach for modeling of multiphase multi-component flow in porous media. J. Comput. Phys. **337**, 275–288 (2017). https://doi.org/10.1016/j.jcp.2017.02.041
12. Wapperom, M., Lyu, X., Voskov, D.: Accurate modeling of near-wellbore effects induced by supercritical CO_2 injection. In: ECMOR 2022 - European Conference on the Mathematics of Geological Reservoirs, pp. 1–13 (2022). https://doi.org/10.3997/2214-4609.202244092
13. Saad, Y.: A flexible inner-outer preconditioned GMRES algorithm. SIAM J. Sci. Comput. **14**, 461–469 (1993). https://doi.org/10.1137/0914028
14. Wallis, J.R., Kendall, R., Little, T.: Constrained residual acceleration of conjugate residual methods. In: SPE Reservoir Simulation Symposium (1985). https://doi.org/10.2118/13536-MS. Society of Petroleum Engineers
15. Tian, X., Blinovs, A., Khait, M., Voskov, D.: Discrete well affinity data-driven proxy model for production forecast. SPE J. **26**(4), 1876–1892 (2021). https://doi.org/10.2118/205489-PA
16. Tian, X., Voskov, D.: Efficient application of stochastic discrete well affinity (DiWA) proxy model with adjoint gradients for production forecast. J. Pet. Sci. Eng. **210** (2022). https://doi.org/10.1016/j.petrol.2021.109911
17. Khait, M., Voskov, D.: Adaptive parameterization for solving of thermal/compositional nonlinear flow and transport with buoyancy. SPE J. **23**(2), 522–534 (2018). https://doi.org/10.2118/182685-PA
18. Lyu, X., Khait, M., Voskov, D.: Operator-based linearization approach for modeling of multiphase flow with buoyancy and cap-

illarity. SPE J. **26**(4), 1858–1878 (2021). https://doi.org/10.2118/205378-PA
19. Khait, M., Voskov, D.: Operator-based linearization for efficient modeling of geothermal processes. Geothermics **74**, 7–18 (2018). https://doi.org/10.1016/j.geothermics.2018.01.012
20. Wang, Y., Voskov, D., Khait, M., Bruhn, D.: An efficient numerical simulator for geothermal simulation: A benchmark study. Applied Energy **264** (2020). https://doi.org/10.1016/j.apenergy.2020.114693
21. Kala, K., Voskov, D.: Element balance formulation in reactive compositional flow and transport with parameterization technique. Comput. Geosci. **24**(2), 609–624 (2020). https://doi.org/10.1007/s10596-019-9828-y
22. Lyu, X., Voskov, D., Rossen, W.R.: Numerical investigations of foam-assisted CO_2 storage in saline aquifers. Int. J. Greenhouse Gas Control **108** (2021). https://doi.org/10.1016/j.ijggc.2021.103314
23. Khait, M., Voskov, D.: GPU-offloaded general purpose simulator for multiphase flow in porous media. SPE Reservoir Simulation Conference, pp. 011–003006 (2017). https://doi.org/10.2118/182663-MS. SPE paper SPE-182663-MS
24. Khait, M., Voskov, D., Zaydullin, R.: High performance framework for modelling of complex subsurface flow and transport applications. In: 17th European Conference on the Mathematics of Oil Recovery (2020). https://doi.org/10.3997/2214-4609.202035188
25. Chen, Y., Voskov, D.: Optimization of CO_2 injection using multiscale reconstruction of composition transport. Comput. Geosci. **24**, 819–835 (2020). https://doi.org/10.1007/s10596-019-09841-8
26. Hoop, S.d., Jones, E., Voskov, D.: Accurate geothermal and chemical dissolution simulation using adaptive mesh refinement on generic unstructured grids. Adv. Water Resour. **154** (2021). https://doi.org/10.1016/j.advwatres.2021.103977
27. de Hoop, S., Voskov, D.V., Bertotti, G., Barnhoorn, A.: An advanced discrete fracture methodology for fast, robust, and accurate simulation of energy production from complex fracture networks. Water Resour. Res. **58**(5) (2022). https://doi.org/10.1029/2021WR030743
28. Novikov, A., Voskov, D.V., Khait, M., Hajibeygi, H., Jansen, J.D.: A collocated finite volume scheme for high-performance simulation of induced seismicity in geo-energy applications. SPE (2021). https://doi.org/10.2118/203903-MS
29. Grospellier, G., Lelandais, B.: The arcane development framework. POOSC '09: Proceedings of the 8th workshop on Parallel/High-Performance Object-Oriented Scientific Computing (2009)
30. Havé, P.: Arcane/ArcGeoSim, a Software Framework for Geosciences Simulation. In: http://orap.irisa.fr/wp-content/uploads/2015/11/ORAP-2015-Have.pdf (2015)
31. Coats, K.H.: An equation of state compositional model. SPE J. (1979). https://doi.org/10.2118/8284-PA
32. Moutte, J., Michel, A., Battaia, G., Parra, T., Garcia, D., Wolf, S.: Arxim, a Library for Thermodynamic Modeling of Reactive Heterogeneous Systems, with Applications to the Simulation of Fluid-rock System. In: 21st Congress of IUPAC. Conference on Chemical Thermodynamic, Tsukuba, Japan (2010)
33. Trenty, L., Michel, A., Tillier, E., Le Gallo, Y.: A sequential splitting strategy for CO_2 storage modelling. In: ECMOR X - 10th European Conference on the Mathematics of Oil Recovery (2006). https://doi.org/10.3997/2214-4609.201402512
34. Bastian, P., Heimann, F., Marnach, S.: Generic implementation of finite element methods in the Distributed and Unified Numerics Environment (DUNE). Kybernetika **46**(2), 294–315 (2010)
35. Sander, O.: DUNE - The Distributed and Unified Numerics Environment. Springer Cham, Springer Nature Switzerland AG (2020)
36. Piatkowski, M., Müthing, S., Bastian, P.: A stable and high-order accurate discontinuous Galerkin based splitting method for the incompressible Navier-Stokes equations. J. Comput. Phys. **356**, 220–239 (2018). https://doi.org/10.1016/j.jcp.2017.11.035
37. Bastian, P.: A fully-coupled discontinuous Galerkin method for two-phase flow in porous media with discontinuous capillary pressure. Comput. Geosci. **18** (2014). https://doi.org/10.1007/s10596-014-9426-y
38. Kempf, D., Heß, R., Müthing, S., Bastian, P.: Automatic Code Generation for High-Performance Discontinuous Galerkin Methods on Modern Architectures. ACM Trans. Math. Softw. **47** (2020). https://doi.org/10.1145/3424144
39. Hintermüller, M., Ito, K., Kunish, M.: The primal-dual active set strategy as a semismooth newton method. SIAM J. Optim. **13** (2002). https://doi.org/10.1137/S1052623401383558
40. Mayer, K.U., Frind, E.O., Blowes, D.W.: Multicomponent reactive transport modeling in variably saturated porous media using a generalized formulation for kinetically controlled reactions. Water Resour. Res., 38–9121 (2002). https://doi.org/10.1029/2001WR000862
41. Seigneur, N., Vriens, B., Beckie, R., zhang, K.: Reactive transport modelling to investigate multi-scale waste rock weathering processes. J. Contam. Hydro. **236**, 103752 (2020). https://doi.org/10.1016/j.jconhyd.2020.103752
42. Mayer, K.U., Amos, R.T., Molins, S., Gérard, F.: Reactive Transport Modeling in Variably Saturated Media with MIN3P: Basic Model Formulation and Model Enhancements. In: Zhang, F., Yeh, G.T., Parker, J.C. (eds.) Groundwater Reactive Transport Models. Bentham Publishers, United Arab Emirates (2012)
43. Molins, S., Mayer, K.U., Amos, R.T., Bekins, B.A.: Vadose zone attenuation of organic compounds at a crude oil spill site - interactions between biogeochemical reactions and multicomponent gas transport. J. Contam. Hydrol. **112**, 15–29 (2010). https://doi.org/10.1016/j.jconhyd.2009.09.002
44. Bea, S.A., Wilson, S.A., Mayer, K.U., Dipple, G.M., Power, I.M., Gamazo, P.: Reactive transport modeling of natural carbon sequestration in ultramafic mine tailings. Vadoze Zone J. **11**(2) (2012). https://doi.org/10.2136/vzj2011.0053
45. Forde, O.N., Mayer, K.U., Cahill, A.G., Mayer, B., Cherry, J.A., Parker, B.L.: Vadose zone gas migration and surface effluxes after a controlled natural gas release into an unconfined shallow aquifer. Vadose Zone J. **17**(1), 180033 (2018). https://doi.org/10.2136/vzj2018.02.0033
46. Henderson, T.H., Mayer, K.U., Parker, B.L., Al, T.A.: Three-dimensional density-dependent flow and multicomponent reactive transport modeling of chlorinated solvent oxidation by potassium permanganate. J. Contam. Hydro. **106**(3), 195–211 (2009). https://doi.org/10.1016/j.jconhyd.2009.02.009
47. Poonoosamy, J., Wanner, C., Alt Epping, P., Àguila, J.F., Samper, J., Montenegro, L., Xie, M., Mayer, K.U., Mäder, U., Van Loon, L.R., Kosakowski, G.: Benchmarking of reactive transport codes for 2D simulations with mineral dissolution-precipitation reactions and feedback on transport parameters. Comput. Geosci., 1337–1358 (2021). https://doi.org/10.1007/s10596-018-9793-x
48. Su, D., Mayer, K.U., MacQuarrie, K.T.B.: MIN3P-HPC: A high-performance unstructured grid code for subsurface flow and reactive transport simulation. Math. Geosci. **53**, 517–550 (2021). https://doi.org/10.1007/s11004-020-09898-7
49. Ben Gharbia, I., Flauraud, E.: Study of compositional multiphase flow formulation using complementarity conditions. Oil & Gas Science and Technology - Rev. IFP Energies nouvelles. **74**(43) (2019). https://doi.org/10.2516/ogst/2019012
50. GEOS. www.geosx.org. [Online; accessed 2023-02-03] (2023)
51. Borio, A., Hamon, F.P., Castelletto, N., White, J.A., Settgast, R.R.: Hybrid mimetic finite-difference and virtual element formulation for coupled poromechanics. Comput. Methods Appl. Mech. Eng. **383**, 113917 (2021). https://doi.org/10.1016/j.cma.2021.113917

52. Cusini, M., White, J.A., Castelletto, N., Settgast, R.R.: Simulation of coupled multiphase flow and geomechanics in porous media with embedded discrete fractures. Int. J. Numer. Anal. Methods Geomech. **45**, 563–584 (2021). https://doi.org/10.1002/nag.3168
53. Bui, Q.M., Hamon, F.P., Castelletto, N., Osei-Kuffuor, D., Settgast, R.R., White, J.A.: Multigrid reduction preconditioning framework for coupled processes in porous and fractured media. Comput. Methods Appl. Mech. Eng. **387**, 114111 (2021). https://doi.org/10.1016/j.cma.2021.114111
54. Bui, Q.M., Osei-Kuffuor, D., Castelletto, N., White, J.A.: A scalable multigrid reduction framework for multiphase poromechanics of heterogeneous media. SIAM J. Sci. Comput. **42**(2), 379–396 (2020). https://doi.org/10.1137/19M1256117
55. Cusini, M., Franceschini, A., Gazzola, L., Gazzola, T., Huang, J., Hamon, F.P., Settgast, R.R., Castelletto, N., White, J.A.: Field-scale simulation of geologic carbon sequestration in faulted and fractured natural formations. Technical report, Lawrence Livermore National Lab.(LLNL), Livermore, CA (United States) (2022)
56. Camargo, J., Hamon, F.P., Mazuyer, A., Meckel, T., Castelletto, N., White, J.A.: Deformation monitoring feasibility for offshore carbon storage in the Gulf-of-Mexico. In: Proceedings of the 16th Greenhouse Gas Control Technologies Conference (GHGT-16) (2022). https://doi.org/10.2139/ssrn.4296637
57. Tang, H., Fu, P., Sherman, C.S., Zhang, J., Ju, X., Hamon, F., Azzolina, N.A., Burton-Kelly, M., Morris, J.P.: A deep learning-accelerated data assimilation and forecasting workflow for commercial-scale geologic carbon storage. Int. J. Greenhouse Gas Control **112**, 103488 (2021). https://doi.org/10.1016/j.ijggc.2021.103488
58. Huang, J., Hao, Y., Settgast, R.R., White, J.A., Mateen, K., Gross, H.: Validation and application of a three-dimensional model for simulating proppant transport and fracture conductivity. Rock Mech. Rock Eng., 1–23 (2022). https://doi.org/10.1016/j.ijggc.2021.103488
59. Costa, A., Cusini, M., Jin, T., Settgast, R.R., Dolbow, J.E.: A multi-resolution approach to hydraulic fracture simulation. Int. J. of Fracture **237**(1), 165–188 (2022). https://doi.org/10.1007/s10704-022-00662-y
60. Orr, F.: Theory of Gas Injection Processes. Tie-Line Publications, Holte (2007)
61. Carrayrou, J., Hoffmann, J., Knabner, P., Kräutle, S., de Dieuleveult, C., Erhel, J., van der Lee, J., Lagneau, V., Mayer, K.U., MacQuarrie, K.T.B.: Comparison of numerical methods for simulating strongly nonlinear and heterogeneous reactive transport problems-the MoMaS benchmark case. Comput. Geosci. **14**, 483–502 (2010). https://doi.org/10.1007/s10596-010-9178-2
62. Barker, J.W., Fayers, F.J.: Transport coefficients for compositional simulation with coarse grids in heterogeneous media. SPE Advanced Technology Series **2**(2), 103–112 (1994). https://doi.org/10.2118/22591-PA
63. Iranshahr, A., Chen, Y., Voskov, D.V.: A coarse-scale compositional model. Comput. Geosci. **18**(5), 797–815 (2014). https://doi.org/10.1007/s10596-014-9427-x

Authors and Affiliations

Etienne Ahusborde[1] · Brahim Amaziane[1] · Stephan de Hoop[2] · Mustapha El Ossmani[1,3] · Eric Flauraud[4] · François P. Hamon[5] · Michel Kern[6,7] · Adrien Socié[8] · Danyang Su[8] · K. Ulrich Mayer[8] · Michal Tóth[9] · Denis Voskov[2,10]

Etienne Ahusborde
etienne.ahusborde@univ-pau.fr

Brahim Amaziane
brahim.amaziane@univ-pau.fr

Stephan de Hoop
S.deHoop-1@tudelft.nl

Mustapha El Ossmani
mustapha.elossmani@univ-pau.fr

Eric Flauraud
eric.flauraud@ifpen.fr

François P. Hamon
francois.hamon@totalenergies.com

Adrien Socié
adrien.socie@cea.fr

Danyang Su
dsu@eoas.ubc.ca

K. Ulrich Mayer
umayer@eoas.ubc.ca

Michal Tóth
michal.toth@iwr.uni-heidelberg.de

Denis Voskov
D.V.Voskov@tudelft.nl

1 Universite de Pau et des Pays de l'Adour, E2S UPPA, CNRS, LMAP, Pau, France

2 Department of Geoscience & Engineering, T.U. Delft, Stevinweg 1, 2628 CN, Delft, Netherlands

3 University of Moulay Ismaïl, L2M3S-ENSAM, 50500 Meknès, Morocco

4 IFP Energies nouvelles, 1 et 4 avenue de Bois-Préau, 92852 Rueil-Malmaison Cedex, France

5 E&P Research & Technology, TotalEnergies, 1201 Louisiana Street, Houston, TX 77002, USA

6 Paris research Center, Inria, 2 rue Simone Iff, 75012 Paris, France

7 CERMICS, ENPC, 77455 Marne-la-Vallée, France

8 Department of Earth, Ocean and Atmospheric Sciences, University of British Columbia, Vancouver, BC, Canada

9 Interdisciplinary Center for Scientific Computing, Heidelberg University, Im Neuenheimer Feld 205, 69120 Heidelberg, Germany

10 Department of Energy Science and Engineering, School of Earth Sciences, Stanford University, 367 Panama Street, Stanford, CA 94305, USA